Available at www.sciencedirect.com

ScienceDirect

journal homepage: www.elsevier.com/locate/he

The interaction of hydrogen jet releases with walls and barriers

*D.B. Willoughby**, *M. Royle*

Health and Safety Laboratory, Buxton, Derbyshire, SK17 9JN, United Kingdom

ARTICLE INFO

Article history:
Received 20 January 2010
Received in revised form
13 May 2010
Accepted 13 May 2010

Keywords:
Jet releases
Barriers
Hydrogen
Jet pressure
Heat flux

ABSTRACT

It has been suggested that separation or safety distances for pressurised hydrogen storage can be reduced by the inclusion of walls or barriers between the hydrogen storage and vulnerable plant or other items. Various NFPA codes [1] suggest the use of 60° inclined fire barriers for protection against jet flames in preference to vertical ones. Work by Sandia National Laboratories [2] included experiments and modeling aimed at characterisation of the effectiveness of barrier walls at reducing hazards.

This paper describes a series of experiments performed in order to compare the performance of 60° barriers with that of 90° barriers. Their relative efficiency at giving protection from thermal radiation and blast overpressure was measured together with the propensity for the thermal radiation and blast overpressure to be reflected back to the source of the leak.

The work was primarily focused on compressed H_2 storage for stationary fuel cell systems, which may be physically separated from a fuel cell system or could be on board such a system. Different orifice sizes were used to simulate different size leaks; all releases were made from storage at 200 bar.

Overall conclusions on barrier performance were made based on the recorded measurements.

1. Introduction

The aim of this work is to provide data on the effectiveness of barrier walls at preventing radiation and physical transport of fire from hydrogen jet flames. The results could be used to inform safety distances for hydrogen storage at fuel cell installations. Using high-pressure release scenarios, the effectiveness of barriers at preventing physical fire spread, radiative heat flux and blast overpressure were investigated.

The work was primarily focused on compressed H_2 on site storage and compression, which may be physically separated from a fuel cell system or could be on board such a system.

The effectiveness of 90° and 60° barriers were investigated and compared with results for free jets.

2. Test facility and set-up

2.1. *Test facility*

The main test facility comprised a purpose-built concrete pad, measuring some 10 m × 10 m inset in a 24 m × 18 m tarmac pad. It also comprised:

* *Corresponding author*. Tel.: +44 1298 218120; fax: +44 1298 218162.
E-mail address: deborah.willoughby@hsl.gov.uk (D.B. Willoughby).

0360-3199/$ – see front matter
doi:10.1016/j.ijhydene.2010.05.077

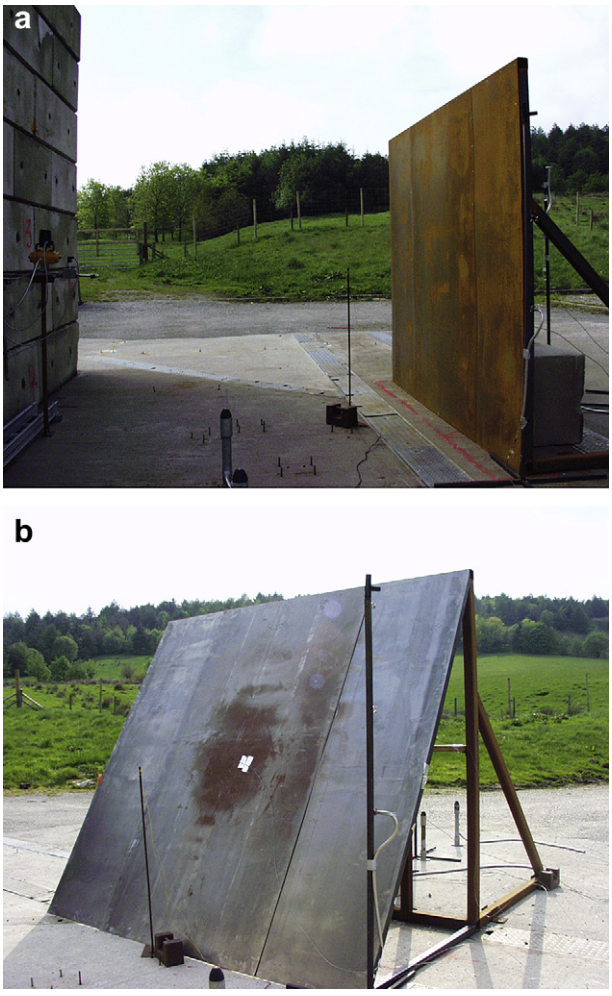

Fig. 1 – (a) 90° barrier; (b) 60° barrier.

- Screw air compressor and associated air drying equipment and air operated gas booster to compress hydrogen
- Two 50-litre storage vessels capable of storing hydrogen at pressure up to 1000 bar
- Pipe work and remotely operated valves to deliver hydrogen to the release point
- Local (15 m from the firing pad) instrument cabin containing the signal conditioning units and data-logging system and control plc
- Remote control room (300 m from the firing pad) with video displays of the trials area and the networked control system
- The release point was situated at 1.2 m above the ground, and the ignition point was located 2 m from the release point

2.2. *Gas supply*

A gas booster was used to charge the two storage vessels with hydrogen to the required release pressure. The hydrogen was delivered to the release point via stainless steel tubing with an internal diameter of 11.9 mm. A series of ball valves was used to control the release; these valves had an internal bore of 9.5 mm. The final release valve was fitted with a modified pneumatic actuator to provide rapid opening and closing of the valve.

2.3. *Release configuration*

Releases of hydrogen were made both with and without flow restrictors in place. The flow restrictors were simple orifices having diameters of 6.4 and 3.2 mm. The flow restrictors consisted of a stainless steel insert 12 mm long with various bores; these were inserted within a modified fitting immediately upstream of the final release valve. All the release functions were controlled remotely.

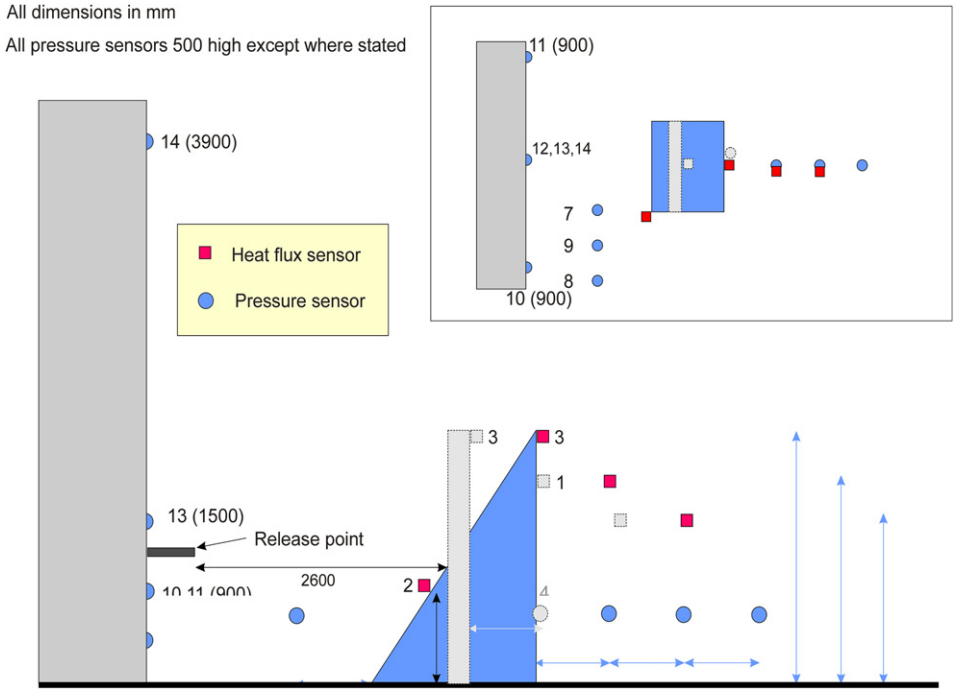

Fig. 2 – Sensor positions (pressure and heat flux) for the 60° and 90° barrier.

Table 1 – Maximum overpressures for 60° and 90° barriers.

Orifice diameter (mm)	Max overpressure (bar) Wall		Max overpressure (bar) Ground		Max overpressure (bar) without barrier Ground	Max overpressure (bar) without barrier Wall
	90° Barrier	60° Barrier	90° Barrier	60° Barrier		
3.2	0.041	0.086	0.033	0.029	0.025	0.035
6.4	0.315	0.438	0.204	0.200	0.191	0.152
9.5	0.422	0.572	0.224	0.288	0.239	0.165

2.4. *Ignition systems*

A pyrotechnic ignition system was used which consisted of a match head igniter, that contained a small amount of pyrotechnic material. The ignition was automatically triggered at a predetermined time during the release by the control system Programmable Logic Controller (PLC).

2.5. *Barrier configuration*

The barriers were constructed of 1.6 mm sheet steel supported on a frame; the dimensions were 3.0 m wide × 2.4 m high. The frames were anchored using a 1-tonne concrete block. The jet stand off was 2.6 m and the jet impacted at the centre of the barrier.

3. Experimental measurements

The following experimental measurements were made:

Overpressure measurement – Two types of pressure sensors were deployed. Kulite ETL-345F-375M Series 40 bara piezo-resistive transducers were used to measure the 'higher' reflected overpressures in the wall and Kulite ETS-IA-375M 17 bara piezo-resistive sensors were used to measure all other overpressures.

The high-pressure Kulite gauges were 40 bar gauges with the data-logging amplification set for a 16 bar range with a measurement error of ±8 mbar. They were factory fitted with shields to protect the sensors against heat and flash light. The lower pressure Kulite gauges were 17 bar gauges with the data-logging amplification set for a 4 bar range. The 17 bar Kulite sensors were factory fitted with an ablative coating to protect the sensors against heat and flash light. All the piezo-resistive sensors were mounted, pointing upwards (except for the wall mounted sensors), in specially made streamlined blocks. Sensors were mounted on blocks fixed into a short length of scaffolding which were bolted into a standard floor fitting fixed to the ground. Sensors were mounted on blocks fixed into the wall.

Heat flux – measurements were made using fast response (50 ms) ellipsoidal radiometers.
Visual records – video records were made at 25 frames per second.
Meteorological measurements – The air temperature, relative humidity, wind speed and direction were measured at the instrument cabin 10 m from the pad using an FT Technologies ultra-sonic anemometer and a Vector Instruments weather station mounted 3.5 m above the ground. This comprised wind speed, wind direction, temperature and humidity measurements. The instruments were connected to the data-logging equipment, allowing recording of the weather conditions to be made during the trials. The data obtained is only indicative, i.e. the instruments were not specifically calibrated for these trials.

4. Release sequence operation

The valve and ignition timing were performed in an automated release sequence by the PLC. The following variables can be set on the system: Release duration – this is the length of time the valve open signal is present at the output and can be set between 0 and 60 000 ms.

Ignition delay – This is the time at which the ignition pulse occurs relative to the valve open signal, i.e. a delay of 0 ms will result in the valve open signal and the ignition pulse occurring at the same time. This can be set between −10 000 and +60 000 ms.

Table 2 – Heat flux recorded with the varying range of orifices.

Heat flux sensor	Radiative heat flux Kw/m^2 3.2 mm restrictor		Radiative heat flux Kw/m^2 6.4 mm restrictor		Radiative heat flux Kw/m^2 9.5 mm restrictor		Radiative heat flux Kw/m^2 6.4 mm restrictor Free Jet
	90° barrier	60° barrier	90° barrier	60° barrier	90° barrier	60° barrier	
HF1	3.85	6.68	4.11	37.5	9.05	27.8	
HF2	39.9	36.7	73.3	82.2	125.7	60.1	65.8
HF3	7.25	43.8	30.0	109.0	32.3	84.9	
HF4	1.72	6.06	7.43	15.0	5.39	11.6	68.5

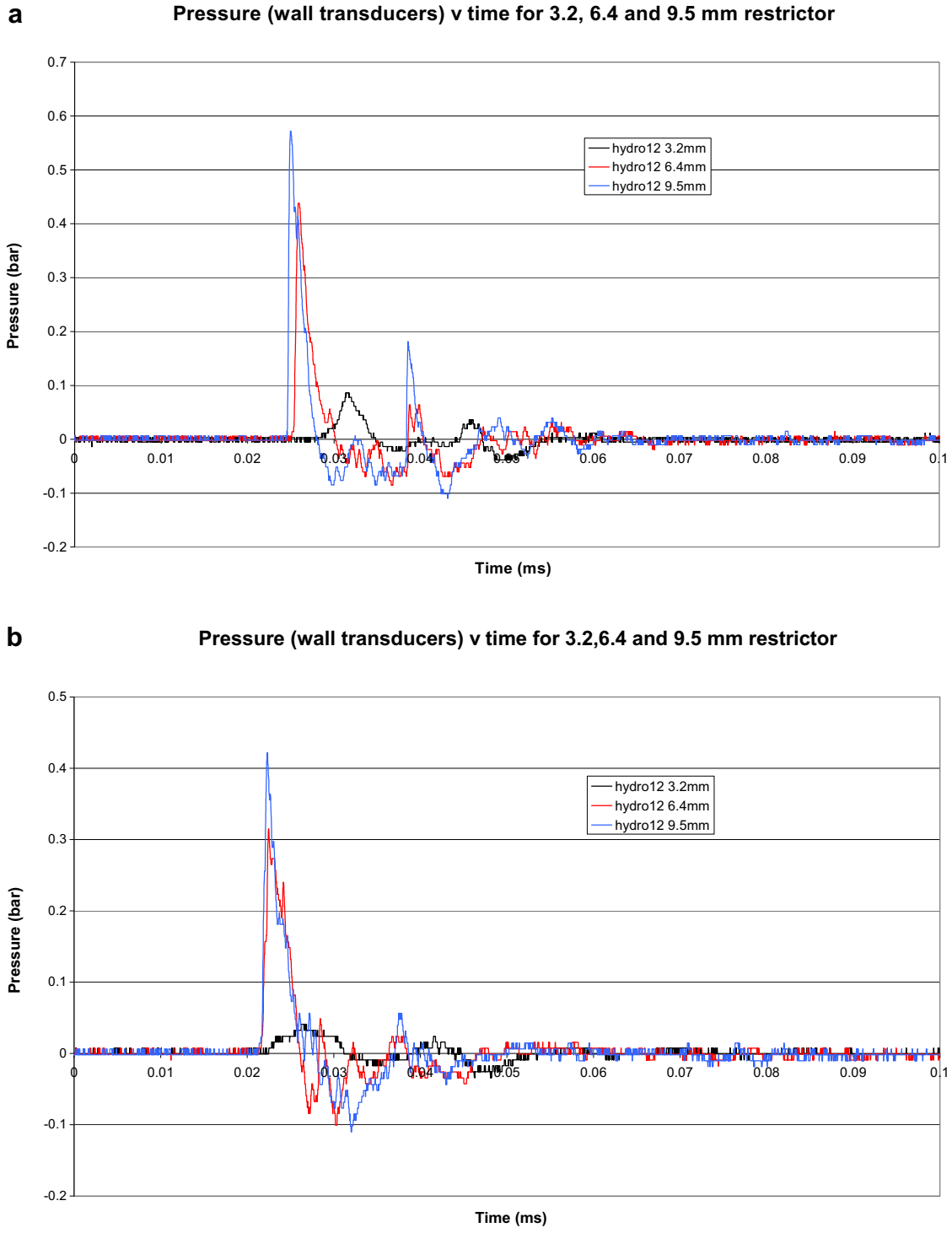

Fig. 3 – (a) Pressure vs time for releases against 90° barrier (wall sensors); (b) Pressure vs time for releases against 60° barrier (wall sensors).

5. Test configurations

5.1. *Barriers*

Two barrier configurations were tested, a 90° barrier see Fig. 1 (a) and a 60° barrier see Fig. 1(b). A test without a barrier was also performed for comparison purposes.

5.2. *Tests performed*

All the tests were performed with hydrogen released at 200 bar horizontally towards the barrier. Six tests were conducted with three different size orifices (three onto a 60° barrier and three onto 90° barrier). A single ignition position, 2 m from the release point and at a height of 1.2 m, was chosen. A single ignition delay of 800 ms and a jet stand off of 2.6 m was used

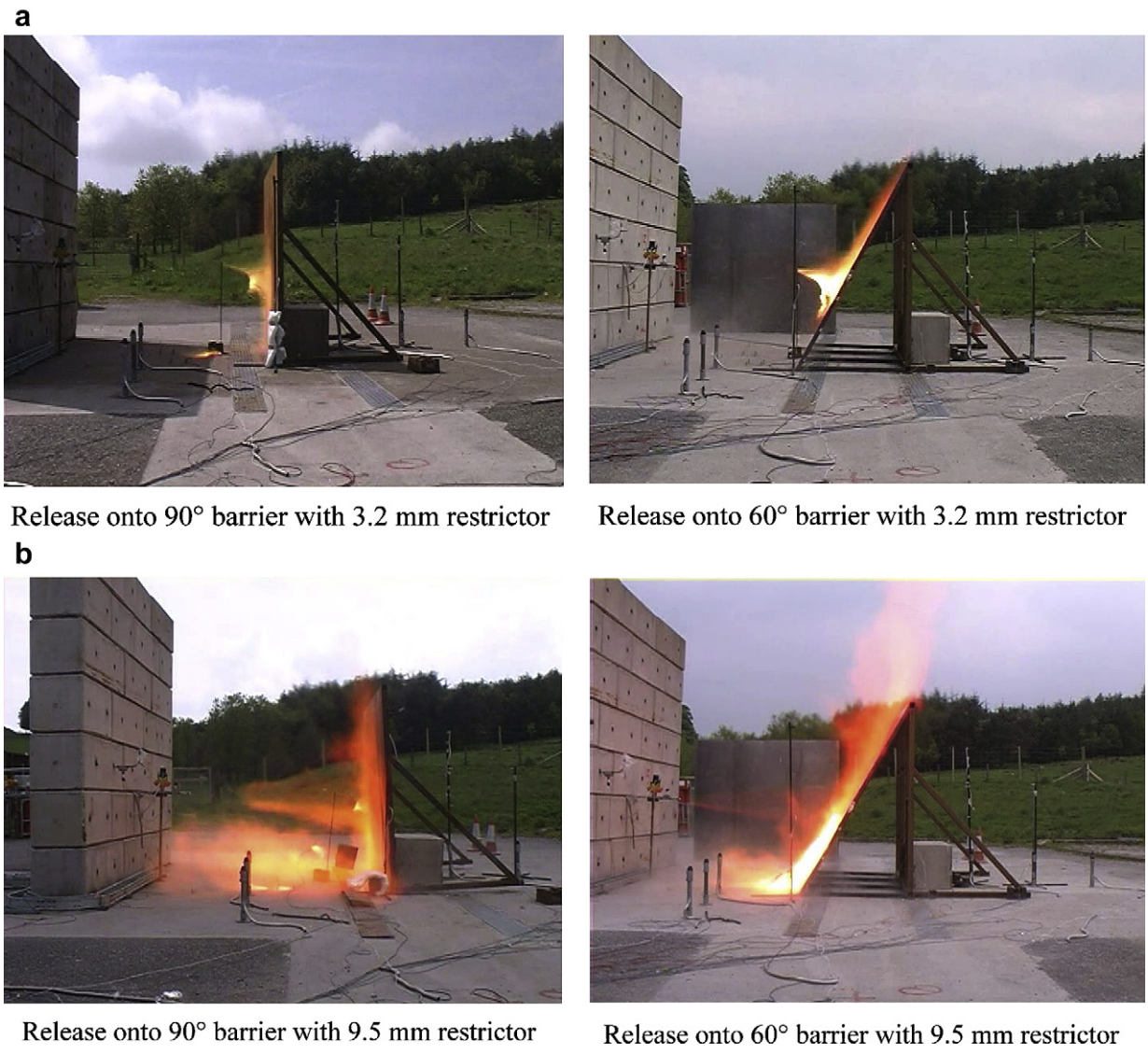

Fig. 4 – (a) Release onto barriers with 3.2 mm restrictor; (a) Release onto barriers with 9.5 mm restrictor.

for all the tests. A 9.5 mm orifice test was conducted without a barrier in place for comparison purposes.

5.3. *Pressure sensors and heat flux meters (60° barrier and 90° barrier)*

The pressure sensors were positioned in front, behind and directly opposite the barrier. The heat flux meters were positioned to the side, top and behind the barrier. Exact locations are shown in Fig. 2.

6. Results

6.1. *Comparison of overpressures measured for releases against a 60° barrier and a 90° barrier*

The maximum overpressures for all tests were recorded on sensor 12, which was located in the wall.

Table 1 gives the maximum overpressures recorded for the 60° and 90° barriers (wall and ground sensors) and with the varying range of orifices.

Overpressure measurements were made on a free jet (no barrier) for comparison purposes.

The pressure versus time traces (maximum overpressure) recorded in the wall with the varying orifices 3.2,

Table 3 – Non-reflected overpressures in front and behind barrier.

Orifice diameter (mm)	Max overpressure (bar)				
	Front of 60° barrier	Behind 60° barrier	Front of 90° barrier	Behind 90° barrier	Without barrier Ground
9.5	0.288	0.094	0.222	0.089	0.239

Table 4 – Comparison of overpressures between 60 and 90° barrier.

Orifice diameter (mm)	Max overpressure (bar)		Max overpressure (bar)	
	Front of 60° barrier	Behind 60° barrier	Front of 90° barrier	Behind 90° barrier
3.2	0.041	0.016	0.029	0.012
6.4	0.200	0.070	0.188	0.045
9.5	0.288	0.094	0.222	0.089

6.4 and 9.5 mm can be seen at Fig. 3(a,b) for the 90° and 60° barrier.

6.2. *Comparison of heat flux measured for releases against a 60° barrier and a 90° barrier*

Heat flux measurements were made on a free jet (no barrier) for comparison purposes. Two sensors were deployed, one at 2.6 m and one at 5.2 m from the release point, (height 1.0 m and 1.5 m from the centre line of jet). The second sensor was placed such that it measured the heat flux from the free jet in the absence of the barrier.

Table 2 gives the heat flux recorded for the tests conducted with the varying range of orifices. The positions of the heat flux meters are:

HF1 behind barrier
HF2 front side of barrier
HF3 top of barrier
HF4 behind barrier

6.3. *Photographic images*

Images of the release impacting onto the barriers with the 3.2 mm and 9.5 mm orifices can be seen in Fig. 4(a,b).

7. Discussion

7.1. *Comparison of overpressures with and without barriers*

In these tests, considerably higher overpressures were measured in the wall for tests with barriers than for those without e.g. 0.572 bar with a barrier and 0.165 bar without a barrier.

While barriers can prevent impingement of flame on the surroundings and have been used as such, (see Figs. 3 and 4) they can create turbulence within the hydrogen jet and this may result in higher overpressures being generated compared with free jets. However, for 9.5 mm jets a significant increase in overpressure due to the presence of the barrier was only seen on the reflected wave.

Higher overpressures were measured on the jet impact side of the barrier, which could have an effect on the integrity of any equipment located in this area. However, overpressures measured behind the barrier were significantly reduced. Table 3 gives non-reflected overpressures in front and behind barrier.

7.2. *Comparison of overpressures between 60° and 90° barriers*

Comparing the overpressures measured on the ground, there is little difference in maximum overpressures (in front) between a 60° and a 90° barrier. The highest overpressure measured was seen on sensor 12 located at the bottom of the wall and with the 60° barrier (0.572 bar). This is probably due to the shorter distance (when compared with the 90° barrier) from the base of the barrier to the base of the wall. Table 4 compares the overpressures in front of and behind the wall for the 60° and the 90° barriers.

7.3. *Comparison of heat flux measured between 60° and 90° barriers*

The 60° barrier resulted in more heat flux being transmitted over the top of the barrier for all restrictor sizes than that for the 90° barrier, e.g. for the 6.4 mm restrictor test the 60° barrier gave 109 kW/m^2 compared to 30 kW/m^2 for the 90° barrier. The sensor located at the side of the barrier measured similar heat fluxes for both 60 and 90° barriers in the 3.2 and the 6.4 mm restricted tests. However, for the 9.5 mm test significantly more heat flux was measured at this position with the 90° barrier (125.7 kW/m^2) i.e. twice as much as for the 60° barrier (60.1 kW/m^2).

The 60° barrier results in significantly more heat flux behind the barrier than for a 90° barrier, up to three times as much for a 9.5 mm restrictor release.

8. Conclusions

(1) The 60° barrier results in more heat flux behind the barrier (up to 3 times more).
(2) The 90° barrier results in more heat flux in front of the barrier, twice the magnitude of that for the 60° barrier.
(3) The 60° barrier results in more heat flux being transmitted around the barrier; a significant reduction in the overpressure produced compared to the 90° barrier was not observed.
(4) The only advantage in using a 60° barrier in preference to a 90° barrier is there is less heat flux reflected back to the leak source.

Acknowledgements

This work was partially funded by the EC as part of the 6th framework Hyper Project.

Joint funding was provided by the United Kingdom Health and Safety Executive.

REFERENCES

[1] Standard for the storage, use, and handling of compressed gases and cryogenic fluids in portable and stationary containers, cylinders, and tanks. NFPA 55; 2005.
[2] Houf W, Schefer R, Merilo E, Grothe M. Evaluation of barrier walls for mitigation of unintended releases of hydrogen. Int J Hydrogen Energy 2010;35(10):4758–75.